

Universal computation by multi-particle quantum walk

Andrew Childs

David Gosset

Zak Webb



UNIVERSITY OF
WATERLOO

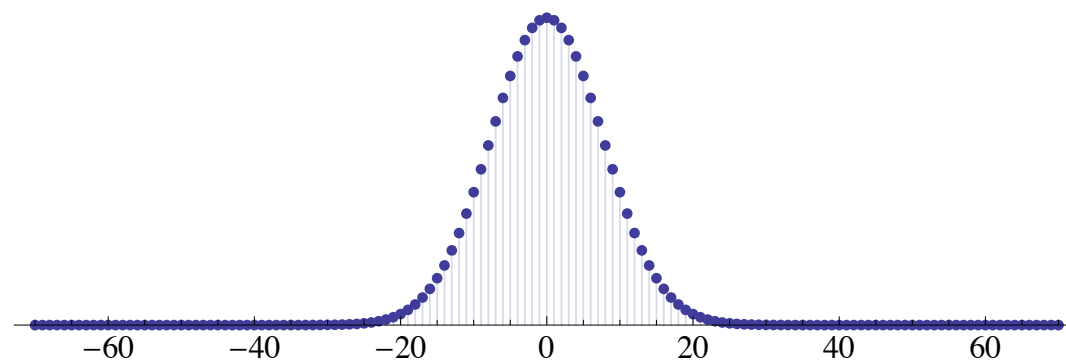
arXiv:1205.3782

Science 339, 791-794 (2013)

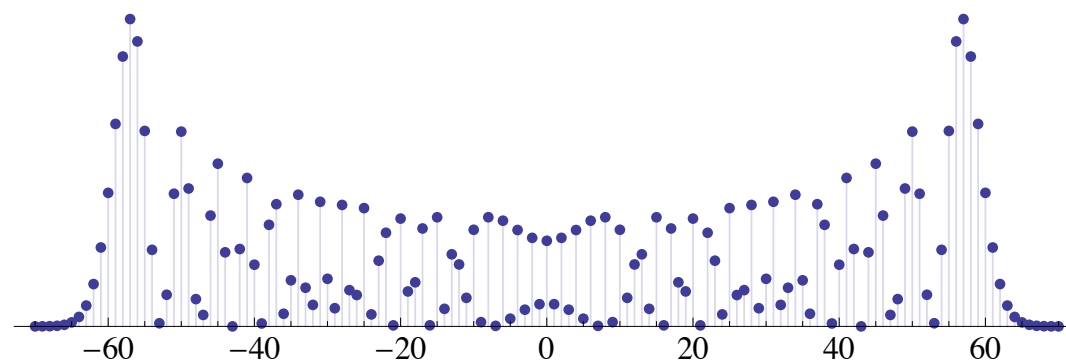
Quantum walk

Quantum analog of a random walk on a graph.

Idea: Replace probabilities by quantum amplitudes.
Interference can produce radically different behavior!



classical



quantum

Quantum walk algorithms

Quantum walk is a major tool for quantum algorithms (especially query algorithms with polynomial speedup).

- Exponential speedup for black-box graph traversal [Childs, Cleve, Deotto, Farhi, Gutmann, Spielman 02]
- Quantum walk search framework [Szegedy 05], [Magniez et al. 06]
 - Spatial search [Shenvi, Kempe, Whaley 02], [Childs, Goldstone 03, 04], [Ambainis, Kempe, Rivosh 04]
 - Element distinctness [Ambainis 03]
 - Subgraph finding [Magniez, Santha, Szegedy 03], [Childs, Kothari 10]
 - Matrix/group problems [Buhrman, Špalek 04], [Magniez, Nayak 05]
- Evaluating formulas/span programs
 - AND-OR formula evaluation [Farhi, Goldstone, Gutmann 07], [ACRŠZ 07]
 - Span programs for general query problems [Reichardt 09]
 - Learning graphs [Belovs 11] → new upper bounds (implicitly, quantum walk algorithms), new kinds of quantum walk search

Universality of quantum walk

A quantum walk can be efficiently simulated by a universal quantum computer.

N -vertex graph
max degree $\text{poly}(\log N)$
efficiently computable neighbors \Rightarrow circuit with
 $\text{poly}(\log N)$ qubits
 $\text{poly}(\log N)$ gates

Conversely, quantum walk is a *universal computational primitive*: any quantum circuit can be simulated by a quantum walk. [Childs 09]

N dimensions
 g gates \Rightarrow graph with
 $\text{poly}(N, g)$ vertices
max degree 3
walk for time $\text{poly}(g)$

Note: The graph is necessarily exponentially large in the number of qubits! Vertices represent basis states.

Quantum walk experiments

Do et al.

Experimental realization of a quantum quincunx by use of linear optical elements

REPORTS

relation between brightness and vertical flow direction (12). This constitutes evidence for a convective flow pattern that transports the energy flux emitted in the penumbra. Other studies show a correlation between intensity and line-of-sight velocities (13), which for sunspots observed outside the center of the solar disk is dominated by the horizontal Evershed flow. This is consistent with our findings, because in the penumbra the horizontal flow velocity is correlated with the vertical flow direction.

Our detailed analysis (8) shows that the spatial scales of the flows providing the major part of the convective energy transport are similar for both undisturbed granulation and penumbra. The primary difference is that there is no preferred horizontal direction for granulation, whereas the energy-transporting flows in the penumbra are distinctly asymmetric: Convective structures are elongated in the radial direction of the sunspot. These properties were already indicated in earlier simulations (5, 6) and suggested as an explanation for the Evershed outflow in (14). The simulation shown here confirms this suggestion and demonstrates the convective nature of a fully developed penumbra.

The horizontal asymmetry of the convective flows is also manifest in the correlation of 0.42 between the corresponding flow component (v_x) and the brightness. We find that the rms of the outflowing velocity component (v_x) in the penumbra is much larger than the transverse component (v_y) (perpendicular to that found by the scale analysis). The total rms velocity profile as a function of depth is very similar to its counterpart for undisturbed granulation, apart from a slightly higher peak value, confirming the physical similarity of convection in granulation and penumbra.

The mass flux and energy flux show similar properties with respect to the length scales and asymmetry (8), indicating that most of the outflowing material emerges, turns over, and descends within the penumbra. In the deeper layers, there is some contribution (of the order of 10 to 20%) to both energy and mass fluxes by the large-scale flow cell surrounding the sunspots.

The analysis of our simulations indicates that granulation and penumbral flows are similar with regard to energy transport; the asymmetry between the horizontal directions and the reduced overall energy flux reflect the constraints imposed on the convective motions by the presence of a strong and inclined magnetic field. The development of systematic outflows is a direct consequence of the anisotropy, and the similarities between granulation and penumbral flows strongly suggest that driving the Evershed flow does not require physical processes that go beyond the combination of convection and anisotropy introduced by the magnetic field. Weaker laterally overturning flows perpendicular to the main filament direction explain the apparent twisting motions observed in some filaments (15, 16) and lead to a weakening of the magnetic field in the flow channels through flux expulsion (6).

Although our simulation of large sunspots is realistic in terms of relevant physics, it does not faithfully reproduce all aspects of the morphology of observed penumbral filaments. The penumbral regions are considerably more extended than in previous local simulations, but they are still somewhat subdued, probably owing to the proximity of what subtended, probably owing to the proximity of the periodic boundaries. The filaments in the inner penumbra appear to be too fragmented, and short, dark lanes along bright filaments (17) form only occasionally, likely a consequence of the still-limited spatial resolution of the simulation. Lastly, the initial condition of the magnetic field underlying the sunspot is quite arbitrary, owing to our ignorance of the subsurface structure of sunspots. Notwithstanding these limitations, the present simulations are consistent with observations of global relations are consistent with observations of global sunspot properties, penumbral structure, and systematic radial outflows. These and earlier simulations (5, 6, 10) suggest a unified physical explanation for umbral dots as well as inner and outer penumbrae in terms of magnetoconvection in a magnetic field with varying inclination. Furthermore, a consistent physical picture of all observational characteristics of sunspots and their surroundings is now emerging.

References and Notes

1. S. K. Solanki, *Astron. Astrophys. Rev.* **11**, 153 (2003).
2. J. H. Thomas, N. O. Weiss, *Annu. Rev. Astron. Astrophys.* **42**, 517 (2004).
3. J. Evershed, *Mon. Not. R. Astron. Soc.* **69**, 454 (1909).
4. J. H. Thomas, N. O. Weiss, *Sunspots and Starspots* (Cambridge Univ. Press, Cambridge, 2008).

Quantum Walk in Position Space with Single Optically Trapped Atoms

Michal Karski,* Leonid Förster, Jai-Min Choi, Andreas Steffen, Wolfgang Alt, Dieter Meschede, Artur Widera*

The quantum walk is the quantum analog of the well-known random walk, which forms the basis for models and applications in many realms of science. Its properties are markedly different from the classical counterpart and might lead to extensive applications in quantum information science. In our experiment, we implemented a quantum walk on the line with single neutral atoms by deterministically delocalizing them over the sites of a one-dimensional spin-dependent optical lattice. With the use of site-resolved fluorescence imaging, the final wave function is characterized by local quantum state tomography, and its spatial coherence is demonstrated. Our system allows the observation of the quantum-to-classical transition and paves the way for applications, such as quantum cellular automata.

Interference phenomena with microscopic particles are a direct consequence of their quantum-mechanical wave nature (1–5). The prospect to fully control quantum properties of atomic systems has stimulated ideas to engineer quantum states that would be useful for applications in quantum information processing, for example, and also would elucidate fundamental questions, such as the quantum-to-classical transition (6). A prominent example of state engineering by controlled multipath interference is the quantum walk of a particle (7). Its classical

counterpart, the random walk, is relevant aspects of our lives, providing insight in fields: It forms the basis for algorithms that describes diffusion processes in physics (8, 9), such as Brownian motion, and is used as a model for stock market. Similarly, the quantum walk is expected

Supporting Online Material
www.sciencemag.org/cgi/content/full/10.1126/science.1173798/DC1
Materials and Methods
SOM Text
Figs. S1 to S4
References
Movies S1 and S2

19 March 2009; accepted 8 June 2009
Published online 18 June 2009;
10.1126/science.1173798
Include this information when citing this paper.
NCAR is sponsored by NSF.

Institut für Angewandte Physik der Universität
straße 8, 53115 Bonn, Germany.
*To whom correspondence should be addressed.
karski@uni-bonn.de (M.K.); widera@uni-

Vol. 22, No. 2/February 2005/J. Opt. Soc. Am. B 499

PRL 100, 170506 (2008)

PHYSICAL REVIEW LETTERS

week ending
2 MAY 2008

Realization of Quantum Walks with Negligible Decoherence in Waveguide Lattices

Hagai B. Perets,^{1,*} Yoav Lahini,¹ Francesca Pozzi,² Marc Sorel,² Roberto Morandotti,³ and Yaron Silberberg¹

¹Faculty of Physics, The Weizmann Institute of Science, 76100 Rehovot, Israel
²Department of Electronics & Electrical Engineering, University of Glasgow, Glasgow G12 8QQ, Scotland, United Kingdom
³Institute National de la Recherche Scientifique, Université du Québec, Varennes, Québec J3X 1S2, Canada
(Received 24 September 2007; published 2 May 2008)

Quantum random walks are the quantum counterpart of classical random walks, and were recently studied in the context of quantum computation. Physical implementations of quantum walks have only been made in very small scale systems severely limited by decoherence. Here we show that the propagation of photons in waveguide lattices, which have been studied extensively in recent years, are essentially an implementation of quantum walks. Since waveguide lattices are easily constructed at large scales and display negligible decoherence, they can serve as an ideal and versatile experimental playground for the study of quantum walks and quantum algorithms. We experimentally observe quantum walks in large systems (~100 sites) and confirm quantum walks effects which were studied theoretically, including ballistic propagation, disorder, and boundary related effects.

DOI: 10.1103/PhysRevLett.100.170506

PACS numbers: 03.67.Lx, 05.40.Fb, 42.25.Dd, 42.50.Xa

In classical random walks, a particle starting from an initial site on a lattice randomly chooses a direction, and then moves to a neighboring site accordingly. This process is repeated until some chosen final time. This process random walk scheme is known to be described by a Gaussian probability distribution of the particle position, where the average absolute distance of the particle from the origin grows as the square root of time. First suggested by Feynman [1] the term *quantum* random walks was defined to describe the random walk behavior of a quantum particle. The coherent character of the quantum particle plays a major role in its dynamics, giving rise to markedly different behavior of quantum walks (QWs) compared with classical ones. For example, in periodic systems, the quantum particle propagates much faster than its classical counterpart, and its distance from the origin grows linearly with time (ballistic propagation) rather than diffusively [2]. In disordered systems, the expansion of the quantum mechanical wave-function can be exponentially suppressed even for infinitesimal amount of disorder, while such suppression does not occur in classical random walks.

In recent years QWs have been extensively studied theoretically [2] and have been used to devise new quantum computation algorithms [3]. Both discrete and continuous time QWs (DQWs; CQWs) [4–6] have been studied. In DQWs the quantum particle hops between lattice sites in discrete time steps, while in CQWs the probability amplitude of the particle leaks continuously to neighboring sites. Experimentally, many methods have been suggested for the implementation of DQWs (see [2]), but only a small scale system consisting of a few states was implemented, using linear optical elements [7]. For CQWs, a few suggestions have been made [8,9], yet only one experimental method has been implemented by realizing a small scale cyclic system (4 states) using a nuclear magnetic resonance system [10]. Such systems are difficult

to scale to much larger configurations. Moreover, even at these very small scales, errors attributed to decoherence have been observed.

Here we suggest a very different implementation of CQWs using optical waveguide lattices. These systems have been studied extensively in recent years [11], but not in the context of QWs and quantum algorithms. We show that these systems can serve as a unique and robust tool for the study of CQWs. For this purpose we demonstrate three fundamental QW effects that have been theoretically analyzed in the QW literature. These include ballistic propagation in the largest system reported to date (~100 sites), the effects of disorder on QWs, and QWs with reflecting boundary conditions (related to Berry's "particle in a box" and quantum carpets [12,13]). Waveguide lattices can be easily realized with even larger scales than shown here (10²–10⁴ sites with current fabrication technologies), with practically no decoherence. The high level of engineering and control of these systems enable the study of a wide range of different parameters and initial conditions. Specifically it allows the implementation and study of a large variety of different show experimental observations of their unique behavior.

The CQW model was first suggested by Farhi and Gutmann [6], where the intuition behind it comes from continuous time classical Markov chains. In the classical random walk on a graph, a step can be described by a matrix M which transforms the probability distribution for the particle position over the graph nodes (sites). The entries of the matrix M_{jk} give the probability to go from site j to site k in one step of the walk. The idea was to carry this construction over to the quantum case, where the *Hamiltonian* of the process is used as the generator matrix. The system is evolved using $U(t) = \exp(-iHt)$. If we start in some initial state $|\Psi_0\rangle$, evolve it under U for a time T and measure the positions of the resulting state, we obtain a

0031-9007/08/100(17)/170506(4)

170506-1

© 2008 The American Physical Society

Multi-particle quantum walk

With many walkers, the Hilbert space can be much bigger.

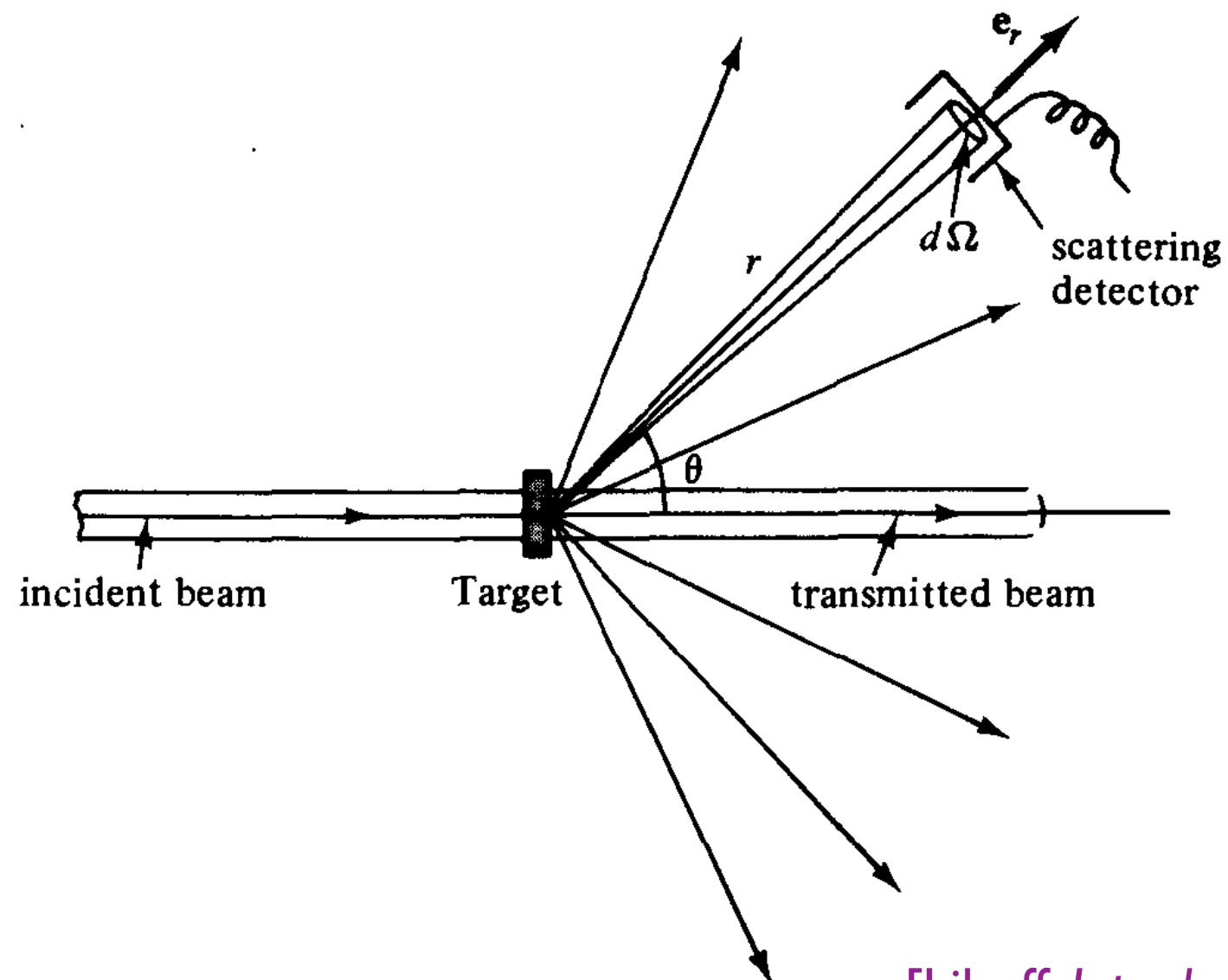
m distinguishable particles on an n -vertex graph: n^m dimensions
(similar scaling for indistinguishable bosons/fermions)

Main result: Any n -qubit, g -gate quantum circuit can be simulated by a multi-particle quantum walk of $n + 1$ particles interacting for time $\text{poly}(n, g)$ on a graph with $\text{poly}(n, g)$ vertices.

Consequences:

- Architecture for a quantum computer with no time-dependent control
- Simulating interacting many-body systems is BQP-hard (e.g., Bose-Hubbard model on a sparse, unweighted, planar graph)

Scattering theory on graphs



Quantum walk

Quantum analog of a random walk on a graph $G = (V, E)$.

Idea: Replace probabilities by quantum amplitudes.

$$|\psi(t)\rangle = \sum_{v \in V} a_v(t) |v\rangle$$

amplitude for vertex v at time t

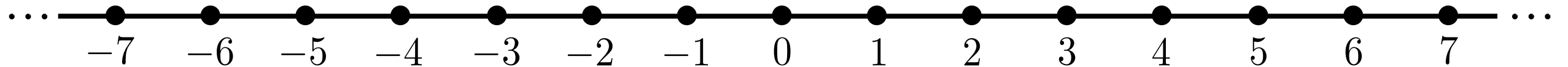
Define time-homogeneous, local dynamics on G .

$$i \frac{d}{dt} |\psi(t)\rangle = H |\psi(t)\rangle$$

Adjacency matrix: $H = \sum_{(u,v) \in E(G)} |u\rangle\langle v|$

Momentum states

Consider an infinite path:



Hilbert space: $\text{span}\{|x\rangle : x \in \mathbb{Z}\}$

Eigenstates of the adjacency matrix: $|\tilde{k}\rangle$ with

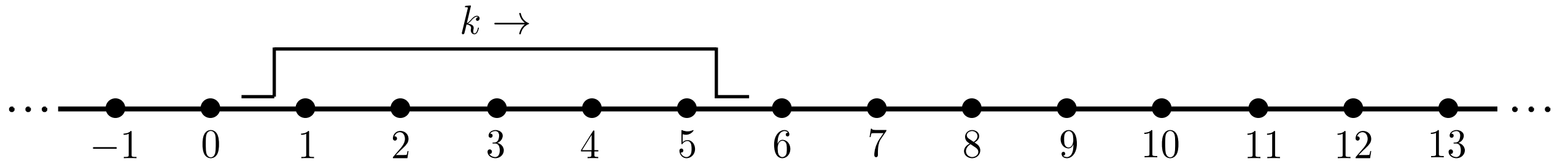
$$\langle x|\tilde{k}\rangle := e^{ikx} \quad k \in [-\pi, \pi)$$

Eigenvalue: $2 \cos k$

Wave packets

A *wave packet* is a normalized state with momentum concentrated near a particular value k .

Example: $\frac{1}{\sqrt{L}} \sum_{x=1}^L e^{-ikx} |x\rangle$ (large L)

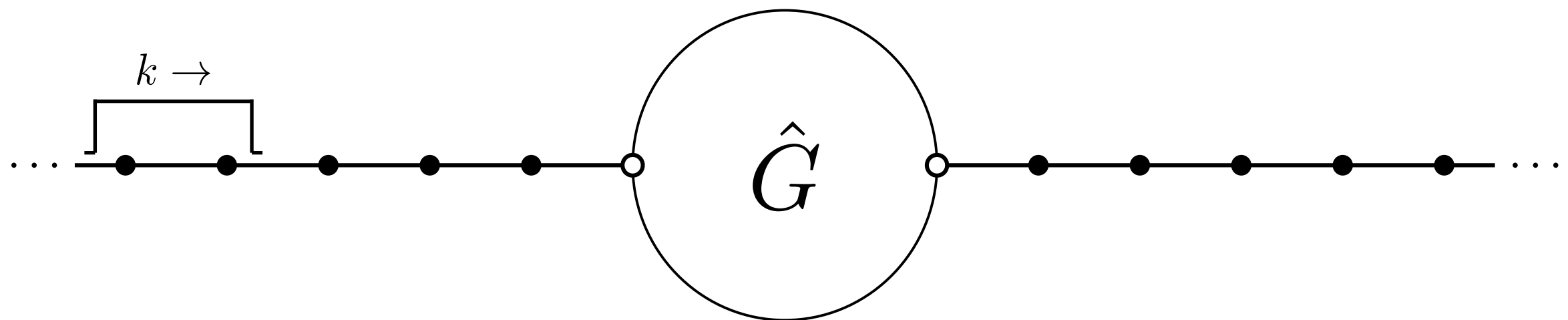


Propagation speed: $\left| \frac{dE}{dk} \right| = 2|\sin k|$

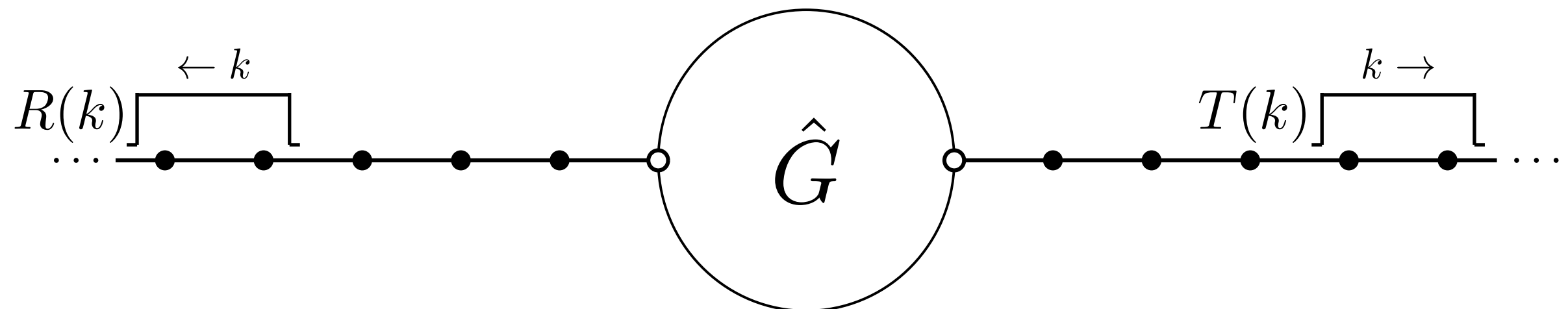
Scattering on graphs

Now consider adding semi-infinite lines to two vertices of an arbitrary finite graph.

Before:

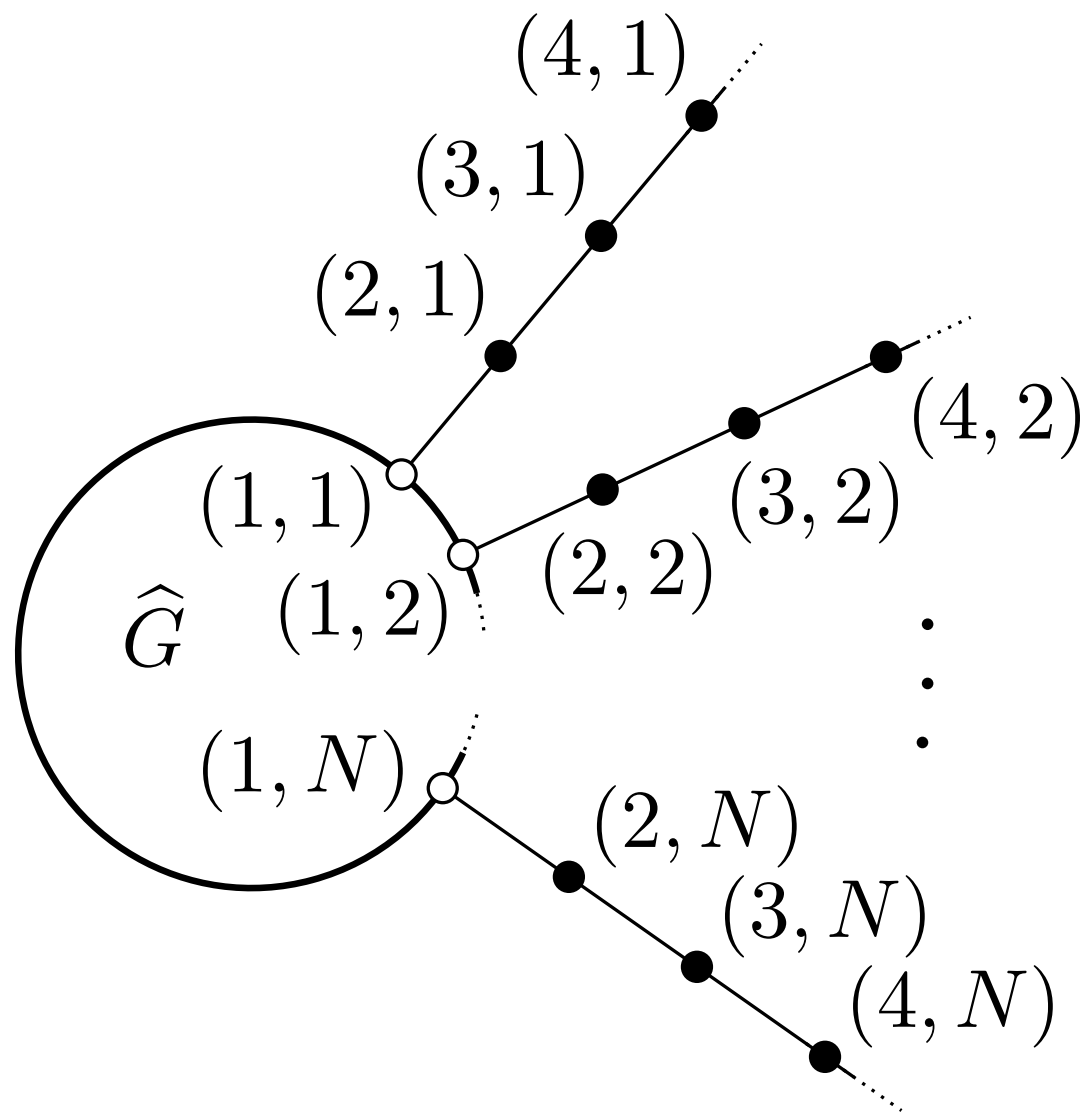


After:



The S-matrix

This generalizes to any number N of semi-infinite paths attached to any finite graph.



Incoming wave packets of momentum near k are mapped to outgoing wave packets (of the same momentum) with amplitudes corresponding to entries of an $N \times N$ unitary matrix $S(k)$, called the S-matrix.

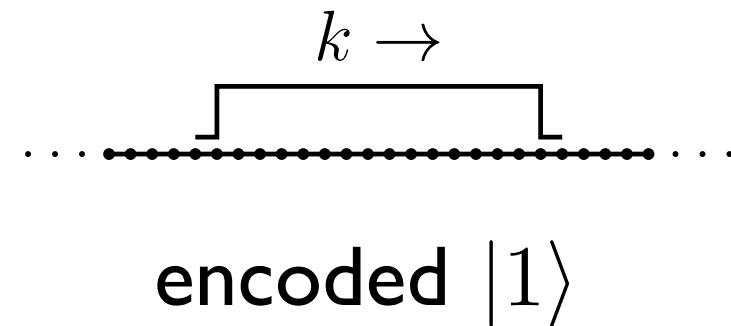
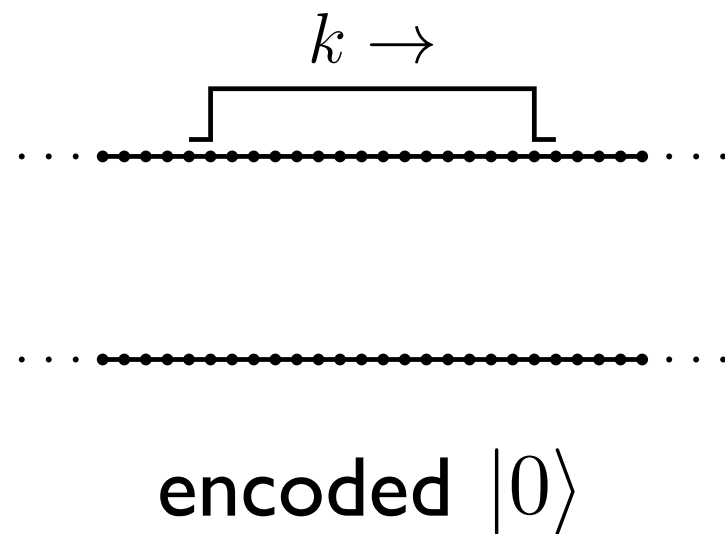
Universal computation

Encoding a qubit

Encode quantum circuits into graphs.

Computational basis states correspond to paths (“quantum wires”).

For one qubit, use two wires (“dual-rail encoding”):

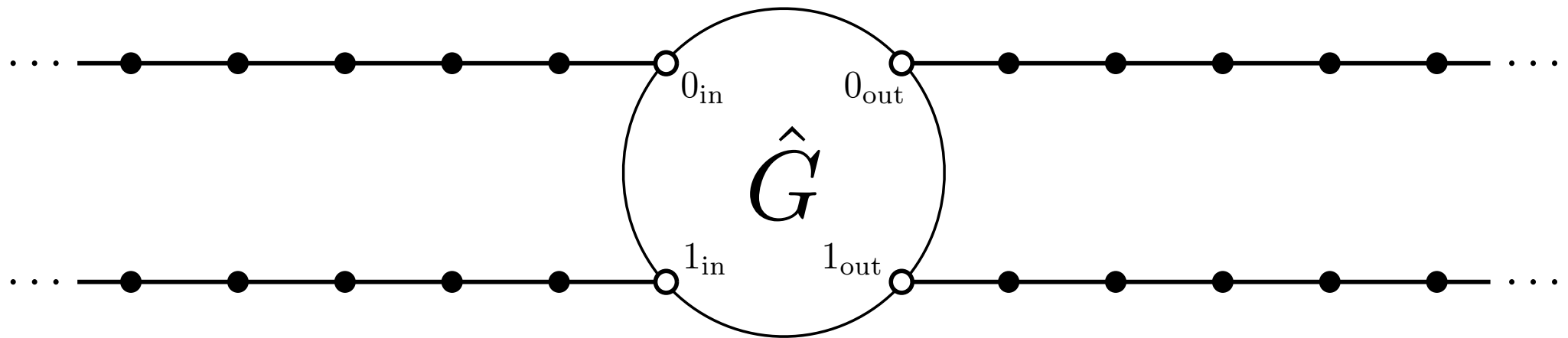


Fix some value of the momentum (e.g., $k = \pi/4$).

Quantum information propagates from left to right at constant speed.

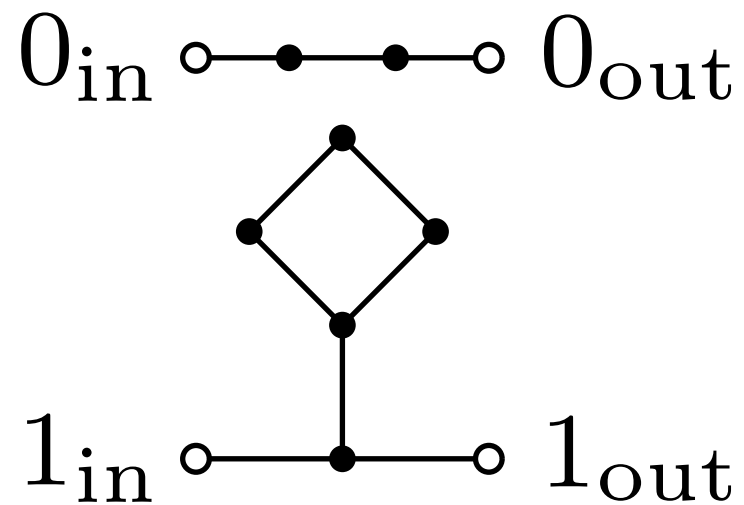
Implementing a gate

To perform a gate, design a graph whose S-matrix implements the desired transformation U at the momentum used for the encoding.

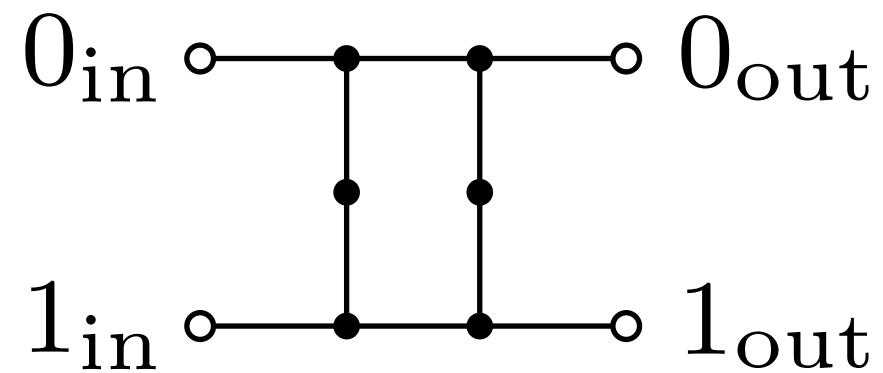


$$S(k) = \begin{pmatrix} 0 & V \\ U & 0 \end{pmatrix}$$

Universal set of single-qubit gates



$$\begin{pmatrix} 1 & 0 \\ 0 & \sqrt{i} \end{pmatrix}$$



$$-\frac{1}{\sqrt{2}} \begin{pmatrix} i & 1 \\ 1 & i \end{pmatrix}$$

momentum for logical states: $k = \pi/4$

Multi-particle quantum walk

With m distinguishable particles:

states: $|v_1, \dots, v_m\rangle \quad v_i \in V(G)$

Hamiltonian: $H_G^{(m)} = \sum_{i=1}^m \sum_{(u,v) \in E(G)} |u\rangle\langle v|_i + \mathcal{U}$

Indistinguishable particles:

bosons: symmetric subspace

fermions: antisymmetric subspace

Many possible interactions:

on-site: $\mathcal{U} = J \sum_{v \in V(G)} \hat{n}_v (\hat{n}_v - 1) \quad \hat{n}_v = \sum_{i=1}^m |v\rangle\langle v|_i$

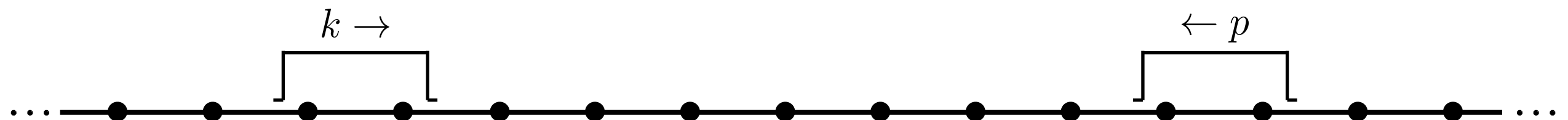
nearest-neighbor: $\mathcal{U} = J \sum_{(u,v) \in E(G)} \hat{n}_u \hat{n}_v$

Two-particle scattering

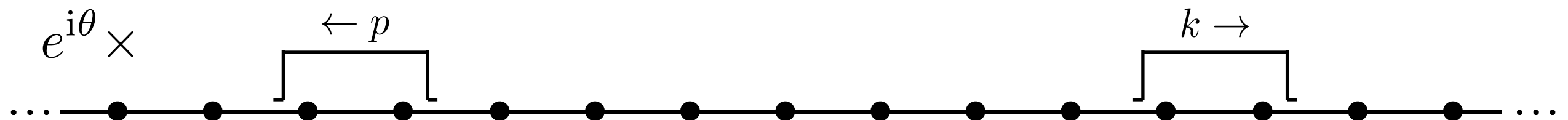
In general, multi-particle scattering is complicated.

But scattering of indistinguishable particles on an infinite path is simple.

Before:



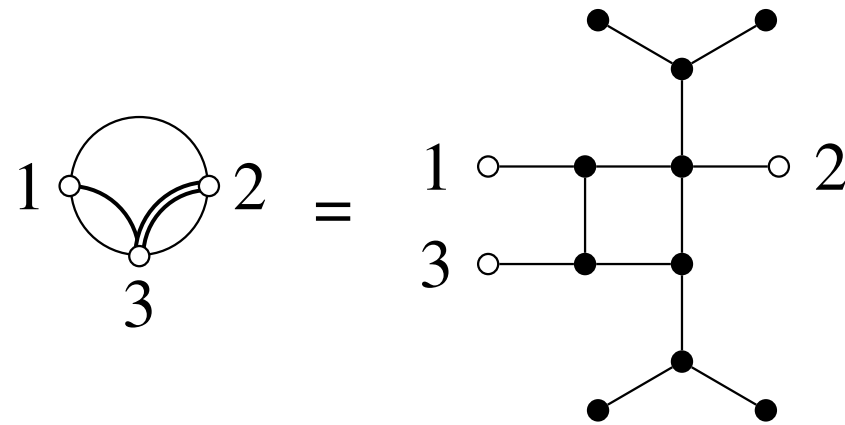
After:



Phase θ depends on momenta and interaction details.

Momentum switch

To selectively induce the two-particle scattering phase, we route particles depending on their momentum.

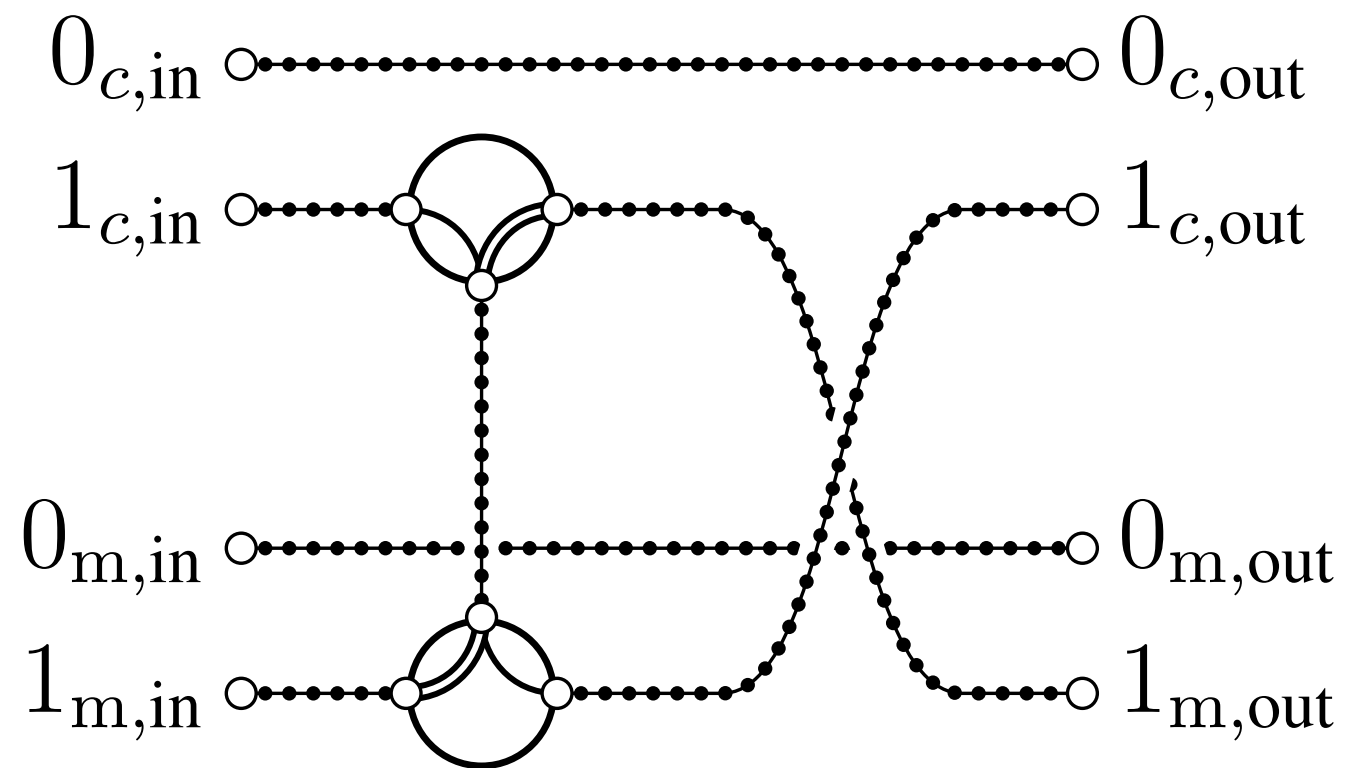


Particles with momentum $\pi/4$ follow the single line.

Particles with momentum $\pi/2$ follow the double line.

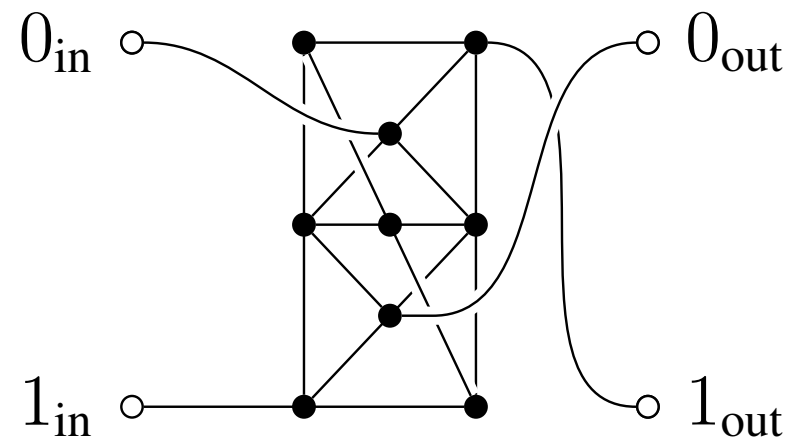
Controlled phase gate

Computational qubits have momentum $\pi/4$. Introduce a “mediator qubit” with momentum $\pi/2$. We can perform an entangling gate with the mediator qubit.



$$C\theta = \begin{pmatrix} 1 & 0 & 0 & 0 \\ 0 & 1 & 0 & 0 \\ 0 & 0 & 1 & 0 \\ 0 & 0 & 0 & e^{i\theta} \end{pmatrix}$$

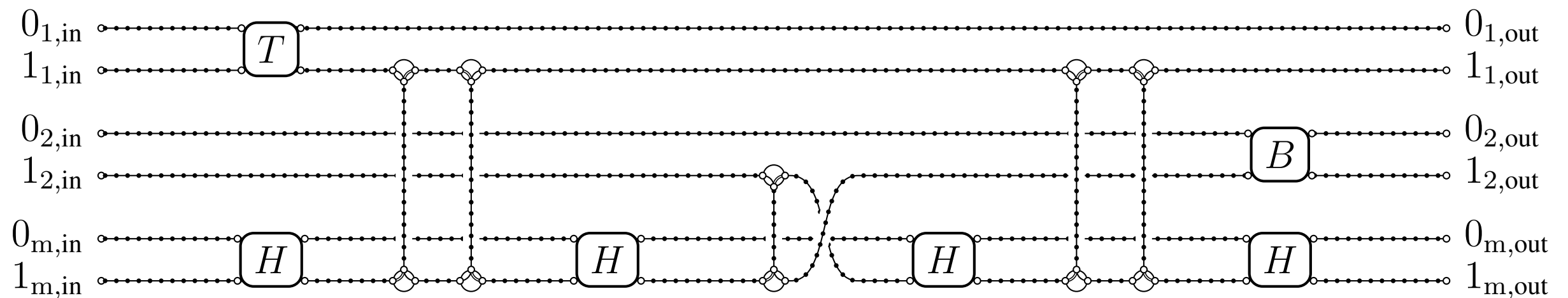
Hadamard on mediator qubit



Error bound

Initial state: each particle is a square wave packet of length L

Consider a g -gate, n -qubit circuit:



$2(n + 1)$ paths, $O(gL)$ vertices on each path

Evolution time $O(gL)$

Total # of vertices $O(ngL)$

Theorem: The error can be made arbitrarily small with $L = \text{poly}(n, g)$.

Example: For Bose-Hubbard model, $L = O(n^{12}g^4)$ suffices.

Open questions

- Improved error bounds
- Simplified initial state
- Are generic interactions universal for distinguishable particles?
- New quantum algorithms
- Experiments
- Fault tolerance